Journal of the Iranian Chemical Society (2019) 16:2765–2776
https://doi.org/10.1007/s13738-019-01738-8

ORIGINAL PAPER

Synthesis and characterization of magnetic poly(acrylic acid) hydrogel fabricated with cobalt nanoparticles for adsorption and catalytic applications

Tariq Mahmood Ansari[1] · Muhammad Ajmal[2] · Sadia Saeed[1] · Hina Naeem[3] · Hafiz Badaruddin Ahmad[1] · Khalid Mahmood[1] · Zahoor H. Farooqi[4]

Received: 29 December 2018 / Accepted: 17 July 2019 / Published online: 24 July 2019

Abstract
The present study aimed to synthesize poly(acrylic acid) hydrogel embedded with magnetic cobalt (Co) nanoparticles and to investigate their potential in adsorption and catalysis. The hydrogel was prepared by facile free radical polymerization reaction and Co nanoparticles were fabricated within hydrogel by reducing Co (II) ions using $NaBH_4$ as reducing agent. Co nanoparticles within hydrogel system imparted magnetic properties to the resulting composite gel and also increased the adsorption capacity. The swelling study of hydrogel was carried out by gravimetric analysis. Different functional groups were identified by Fourier Transform Infrared Spectroscopy and Transmission Electron Microscopy analysis was done to investigate dispersion of Co nanoparticles in hydrogel. The bare hydrogel along with Co nanoparticles loaded gel were tested as adsorbent systems for the removal of a cationic dye (methylene blue) from aqueous solution. 95% removal of methylene blue was achieved with a highest adsorption capacity of 836.5 mg/g of adsorbent. The famous adsorption isotherms were used to evaluate adsorption data. Results showed that Freundlich isotherm model was followed with R^2 value of 0.95. The hydrogel was also used for catalytic reduction in a toxic pollutant, i.e., 4-nitrophenol. Experimental data for 4-nitrophenol reduction followed pseudo first order kinetics model. Activation energy and apparent rate constant were calculated as 9.24 kJ/mol and 0.24 min^{-1}, respectively. Recycling of the magnetic poly(acrylic acid) hydrogel fabricated with Cobalt nanoparticles was carried out for four consecutive cycles and no significant loss in catalytic activity was observed.

Keywords Magnetic hydrogel · Adsorption · Catalysis · Methylene blue · 4-Nitrophenol

Introduction

Hydrogels, the three dimensional polymeric networks which have the ability to swell by absorbing significant amount of water without structural breakdown [1]. Due to potential applications in targeted drug delivery [2, 3], wound dressing [4], tissue engineering [5] reactors for controlled synthesis of various nanoparticles [6, 7], catalysis [8–11], water purification and separation [12, 13], etc., hydrogels have achieved a significant position in the field of material science in the last few decades. Such a wide spectrum of applications of hydrogels stems from the variety of functional groups such as –COOH, $–NH_2$, –SH, etc. present in the hydrogel networks. Diverse functional groups present on polymer chains in hydrogel networks also possess ability to attract charged metal ions via electrostatic attractions. This characteristic of hydrogel networks is advantageous in loading various metal ions into the hydrogel networks followed by their conversion into metal nanoparticles by in situ chemical reduction [7, 14]. Additionally, these three dimensional hydrogel networks also provide stability to in situ prepared nanoparticles in terms of their controlled aggregation. The mesh size of hydrogel network is also a critical parameter in controlling size as well as loading amount of in situ prepared

✉ Muhammad Ajmal
m.ajmal65@yahoo.com

1 Institute of Chemical Sciences, Bahauddin Zakariya University, Multan 60800, Pakistan

2 Department of Chemistry, University of Education, Attock Campus, Attock 43600, Pakistan

3 Department of Chemistry, Quaid-i-Azam University, Islamabad 45320, Pakistan

4 Institute of Chemistry, University of the Punjab, New Campus, Lahore 54590, Pakistan

nanoparticles. It can further be controlled by controlling the cross-linking network within hydrogel system [15]. Nature of functional groups in hydrogel networks also controls loading amount of nanomaterial, in addition to cross-linking density. So, the uniform cross-linking density along with uniform distribution of functional groups throughout the hydrogel networks imparts hydrogel with uniform mesh size. Such a hydrogel system can be used as a matrix for synthesis of nanoparticles of homogeneous shape and size [16, 17]. Due to the above-mentioned advantages, hydrogels are being widely used for the preparation of various nanostructured materials with controlled morphology. For example, Farooqi et al. [18] have prepared poly(*N*-isopropylacrylamide-co-acrylic acid) [p(NiPA-co-AAc)] hydrogel for the fabrication of silver nanoparticles. Well dispersed and almost homogenous silver nanoparticles were obtained demonstrating that applied hydrogel has acted as very good stabilizing agent. Silver nanoparticles loaded hydrogel showed excellent catalytic activity test for the 4-nitroaniline reduction. Hydrogels containing carboxylic functional groups were prepared by Ajmal et al. [19] and used as reactor for the in situ synthesis of transition metal nanoparticles such as copper (Cu), cobalt (Co) and nickel (Ni). Nanoparticles without aggregation were obtained reflecting the potential of these templates as stabilizers. The resultant composite hydrogels fabricated with Cu, Co, and Ni nanoparticles exhibited catalytic activity for nitro aromatic compounds reduction. The utility of hydrogel networks as reactors for the metal nanoparticles fabrication have also been testified by Sahiner et al. [20]. They prepared vinyl phosphonic acid (VPA)-based hydrogel and employed it as a reactor for the fabrication of magnetic iron oxide nanoparticles in situ. Apart from their applications in the controlled synthesis of nanostructured materials, hydrogels with suitable chemical composition and hierarchy could have high potential to act as adsorbent for the removal of many different pollutants from different mediums. The adsorption capabilities of hydrogels with different compositions have been explored by many research groups. For example, hydroxylamine and carboxylic group containing hydrogels have been reported to remove a variety of pollutants from contaminated water [21]. Similarly, chitosan-based hydrogels were used as adsorbent by Kang et al. [22] for methylene blue removal from water.

Due to versatile applications of hydrogels; to act as adsorbent/superabsorbent, to act as template for architecting the metal nanoparticles of controlled shape and size, the ability of as-prepared hydrogel-metal nanoparticle composite to act as a catalyst for various catalytic reactions, it is pertinent to design hydrogels with different chemical composition and to explore their possible applications. In this context, we have prepared poly(acrylic acid) [p(AAc)] hydrogel in bulk dimension by a facile route and used it as template for Co nanoparticles synthesis. The prepared hydrogel and corresponding composite was applied as adsorbent for methylene blue (MB) removal from water and also as a catalyst for 4-nitrophenol (4-NP) reduction. The Influence of various factors on adsorption and catalytic reaction were evaluated. p(AAc) contains large number of carboxyl groups. These carboxyl groups can be deprotonated to negatively charged carboxylate groups which can be employed to load huge amounts of oppositely charged moieties. If p(AAc) is prepared in the form of three dimensional network with low cross-linking density then it can hold very large amounts of positively charged substances such as metal ions or dye and this was the motivation behind the preparation of this hydrogel system. A successful effort to prepare the p(AAc) bulk hydrogel was carried out by Seven and Sahiner [23] but they adopted an indirect, long and hectic rout where poly(acrylamide) was first prepared and then amide groups were modified to carboxyl groups. Therefore, the preparation of p(AAc) hydrogel via an easy, short and economical rout has become very important. The present work demonstrates the synthesis of lightly cross linked p(AAc) bulk hydrogel via a single step process and its potential as reactor for the synthesis of metal nanoparticles as well as adsorptive removal of water pollutants. The catalytic potential of cobalt nanoparticles containing hydrogel has also been investigated.

Experimental

Materials

Acrylic acid (AAc, 98%) purchased from Alfa Aesar was utilized as monomer. *N*, *N*′-methylenebisacrylamide (MBA, 99%) purchased from sigma Aldrich was used as cross-linker. Ammonium persulfate (APS, 99%) purchased from sigma Aldrich) and *N*, *N*, *N*′, *N*′-tetramethylethylene-1,2-diamine (TEMED, 98%) purchased from Merck were used as initiator and accelerator, respectively. Neutralization of p(AAc) hydrogel was carried out with sodium hydroxide (NaOH, 98%) purchased from Aldrich. As a source of Co (II) ions, Cobalt (II) chloride hexahydrate ($CoCl_2{\cdot}6H_2O$, 99%) of Sigma Aldrich was used and sodium borohydride ($NaBH_4$, 98%) of sigma Aldrich was employed as reducing agent for the Co nanoparticles preparation and for 4-NP reduction. Distilled water was used as solvent for the hydrogel preparation, other aqueous solutions, and cleansing.

Synthesis of p(AAc) hydrogel

Free radical polymerization method was utilized for the preparation of p(AAc) hydrogel matrix. For polymerization, distilled water was used as solvent and the reaction was carried out at room temperature. First of all, aqueous

solutions of monomer, cross-linker and initiator were prepared in separate glass containers by dissolving 0.028 mol of AAc in 2 ml distilled water, 0.0432 g of MBA (0.5 mol% of monomer) in 1 ml distilled water, and 0.032 g of APS (0.5 mol% of monomer) in 1 ml distilled water. The prepared aqueous solutions were mixed together. A 100 µL of TEMED was used as accelerator. The reaction mixture, after shaking well to get homogenized was transferred into plastic straws. The AAc was allowed to cross-link and polymerize simultaneously in plastic straws at room temperature for about 24 h. Within 24 h, a semi solid type hydrogel was produced. As the polymerization time was completed, the prepared hydrogel was removed out from the plastic straws. The long cylindrical shaped hydrogel was then divided into small pieces and placed in distilled water to get rid of impurities and unreacted materials from the prepared hydrogel networks. For cleanliness from impurities or unreacted materials, hydrogel was kept in distilled water for 3 days. During the cleanliness time period, water of cleansing medium was regularly replaced twice a day. After cleanliness, the hydrogel was removed from water and dried in the oven. The dried hydrogel was stored at room temperature in an air tight container.

Cobalt nanoparticles synthesis within p(AAc) hydrogel

First of all, prepared hydrogel was treated with NaOH for neutralization and then filtered out, washed and cleansed by using distilled water and then by acetone and oven dried for further use. A 500 ppm aqueous Co (II) solution was prepared using $CoCl_2{\cdot}6H_2O$ as a precursor of Co (II). 0.5 g of prepared hydrogel was added into 250 ml Co (II) solution and stirred for overnight followed by the separation of Co (II) loaded hydrogel and its washing with distilled water and then oven dried at 60 °C. A certain quantity of Co (II) ions loaded hydrogel (0.03 g) was treated with 0.19 g of $NaBH_4$ in aqueous medium for conversion of Co (II) ions into Co nanoparticles under continuous stirring till hydrogen gas evolution was stopped. At the end, the prepared composite hydrogel was filtered out, washed with distilled water at least three times, dried in oven and used further for characterization.

Characterization

Fourier Transform Infrared (FT-IR) spectra were recorded on Nexus 870 FT-IR spectrometer in transmission mode to identify the different functional groups in the hydrogel and hydrogel composite. The scan range for FT-IR spectra was kept as 4000–650 cm^{-1}. For visualization of Co nanoparticles in the p(AAc) hydrogel networks, Transmission electron microscopy (TEM) was used. TECANI-G-20-TEM instrument was used to take TEM image. The UV–Visible 1800 ENG240V, SOFT spectrophotometer with wavelength range between 200 and 800 nm was used for analyzing the catalytic activity of p(AAc)-Co hydrogel composite by carrying out 4-NP reduction and also to find out the adsorption of MB onto the p(AAc) hydrogel and p(AAc)-Co hydrogel composite.

Catalytic activity of composite hydrogel

Composite hydrogel was evaluated as a catalyst system for 4-NP reduction reaction. For observation of catalytic test, the reaction mixture was constituted with 50 ml solution of 0.001 M 4-NP, 0.19 g of $NaBH_4$ and 0.03 g of Co nanoparticle loaded hydrogel. The reaction was studied in a temperature controlled oil bath to maintain constant temperature atmosphere throughout the reaction process. During the reaction, at specific time intervals, aliquots of about 0.5 ml were taken from the reaction mixture, diluted with 10 ml distilled water and then used to record absorbance with UV–Visible spectrophotometer. The absorbance value at 400 nm was observed to decrease with the passage of time and this is an indication of progress of reaction. For the determination of activation energy (E_a) the catalytic test was studied at 30 and 60 °C while none of the other parameters was changed.

Adsorption study

The potential of prepared bare and composite hydrogel to be used as adsorbent was investigated by carrying out the adsorption studies of MB from water. To a 100 ml MB solution with different concentration ranging from 50 to 800 ppm, 0.05 g of hydrogel was added as adsorbent and the solution was stirred at 100 rpm. The adsorption process was performed at room temperature with constant magnetic stirring. 1 ml sample was removed from the reaction mixture at different times. Then, these samples were diluted with distilled water about 10 to 15 times. This dilution was related with initial concentration. The amount of MB adsorbed on hydrogel was measured by UV–Visible spectrophotometer in terms of measurement of absorbance of MB solution at its absorption maxima of 664 nm. The adsorption capacity of composite hydrogel was studied by using its 0.05 g as an adsorbent in 100 ml MB solution having concentration of 250 ppm.

Results and discussion

p(AAc) hydrogel synthesis and its use for cobalt nanoparticles synthesis

Synthesis of p(AAc) hydrogels was accomplished via free radical polymerization. The molecules of monomer, initiator

and cross-linker were allowed to react simultaneously in the reaction medium. In such reactions, the accelerator helps to produce highly reactive sulfate radicals from APS. These reactive radicals then react with monomers and cross-linkers. The monomers react with each other and with the cross-linkers. As a result, the growth of polymer chains and their cross-linking takes place simultaneously and a three dimensional polymeric network is prepared. p(AAc) contains large numbers of carboxylic groups (–COOH). These groups were deprotonated by treating with NaOH to obtain negatively charged carboxyl (COO^-) groups and the deprotonated p(AAc) hydrogel was utilized as a reactor for the synthesis of Co nanoparticles. Figure 1 shows the schematic representation for Co nanoparticles preparation in the matrices of p(AAc) hydrogel along with their physical states at each step of reaction. The bare p(AAc) hydrogel was off-white colored as shown in digital camera image 1 in Fig. 1. On placing the neutralized p(AAc) hydrogel in aqueous solution of Co (II) ions, the Co (II) ions rushed into p(AAc) hydrogel networks due to the electrostatic attractive forces between Co (II) positive ions and negatively charged COO^- groups and were entangled in the hydrogel networks. The change in color from off-white to pink as shown by digital camera image 2 was the indication of loading of Co (II) ions in hydrogel. When the Co (II) loaded p(AAc) hydrogel was treated with $NaBH_4$ then Co nanoparticles were formed and the color of the product turned black as depicted by digital camera image 3.

Characterization

The ability of p(AAc) hydrogel to swell was studied in terms of measuring the amount of water captured by a piece of hydrogel placed in water with time. The increase in weight of p(AAc) hydrogel was measured gravimetrically with time. This was carried out by taking out the swollen hydrogel piece from the swelling medium, measuring its weight and then inserting it back into the distilled water until mass of the hydrogel became constant. And this was done three times to get an average value. Percentage swelling is calculated by formula given by Eq. (1)

$$S\% = \left[\left(M_t - M_\mathrm{d}\right)/M_\mathrm{d}\right] \times 100 \quad (1)$$

Here, M_t represents hydrogel mass in swollen state at time t and M_d is its mass in dried form before inserting it in water. Figure 2 shows percent swelling with the passage of time. The maximum swelling percent was 300 and it was achieved in 200 min. The FT-IR spectra of the prepared p(AAc) hydrogel and composite is shown in Fig. 3. Formation of p(AAc) hydrogel was indicated by the absence of absorption band in the wavenumber region of 1640 to 1680 cm^{-1} where characteristic peaks of C=C appears [24]. The absence of absorption peak in this region represents that almost all C=C double bonds were consumed and hence monomers were polymerized. The band that appeared at 3400 cm^{-1} was due to –OH group. The absorption band of C=O (carbonyl group) of carboxylic acid was found at 1200 cm^{-1}. The $–CH_2$ groups of p(AAc) hydrogel were indicated by absorption band at 1500 cm^{-1}. A similar pattern of absorption bands with a slight shifts was observed for p(AAc)-Co composite. The shifts in absorption peaks in case of composite hydrogel can occur due to interaction between Co nanoparticles and functional groups in polymer hydrogel networks [25]. The Co nanoparticles prepared inside the p(AAc) hydrogel networks were seen by TEM. Figure 4 represents Co nanoparticles embedded in the p(AAc) hydrogel visualized by TEM. It can be seen from the TEM image that no aggregates of Co nanoparticles were formed within the p(AAc) hydrogel. The image also shows that Co nanoparticles were distributed throughout the p(AAc) hydrogel. The presence of well dispersed nanoparticles in p(AAc) hydrogel networks reveals the fact that the prepared p(AAc) hydrogel has potential to be used as reactor medium for the preparation of almost spherical shaped Co nanoparticles and as stabilizing agent to obstruct the aggregation of the prepared nanoparticles. Due to strong paramagnetic properties of Co nanoparticles, the Co nanoparticles prepared p(AAc)-Co hydrogel composite showed magnetic behavior which has been represented in Fig. 5 by the attraction of p(AAc)-Co hydrogel composite toward the applied magnetic field. Camera images 5 (a) and (c) represent the p(AAc)-Co hydrogel composite in dried form and suspended in water, respectively. The camera images (b) and (d) demonstrate that when magnetic field was applied, the particles of p(AAc)-Co composite were attracted toward the magnet bar from their dried state as well as from aqueous medium, respectively. The hydrogel composite particles were attached with the wall of the glass vial near the magnet bar irrespective of their presence in dried form or in water. This ability of p(AAc)-Co composite to response the externally applied magnetic field can be potentially used for controlling the adsorption and catalytic rates as well as for the separation of this adsorbent/catalyst from reaction mixture upon the completion of its given task.

Applications

The applications of bare and composite hydrogel prepared in this work were studied in two different fields; in catalysis and in adsorption. The ability of these hydrogels to act as adsorbents was testified by applying them as adsorbent for the elimination of MB from water. The catalytic activity was testified by applying p(AAc)-Co hydrogel composite for the catalytic reduction of 4-NP into 4-AP.

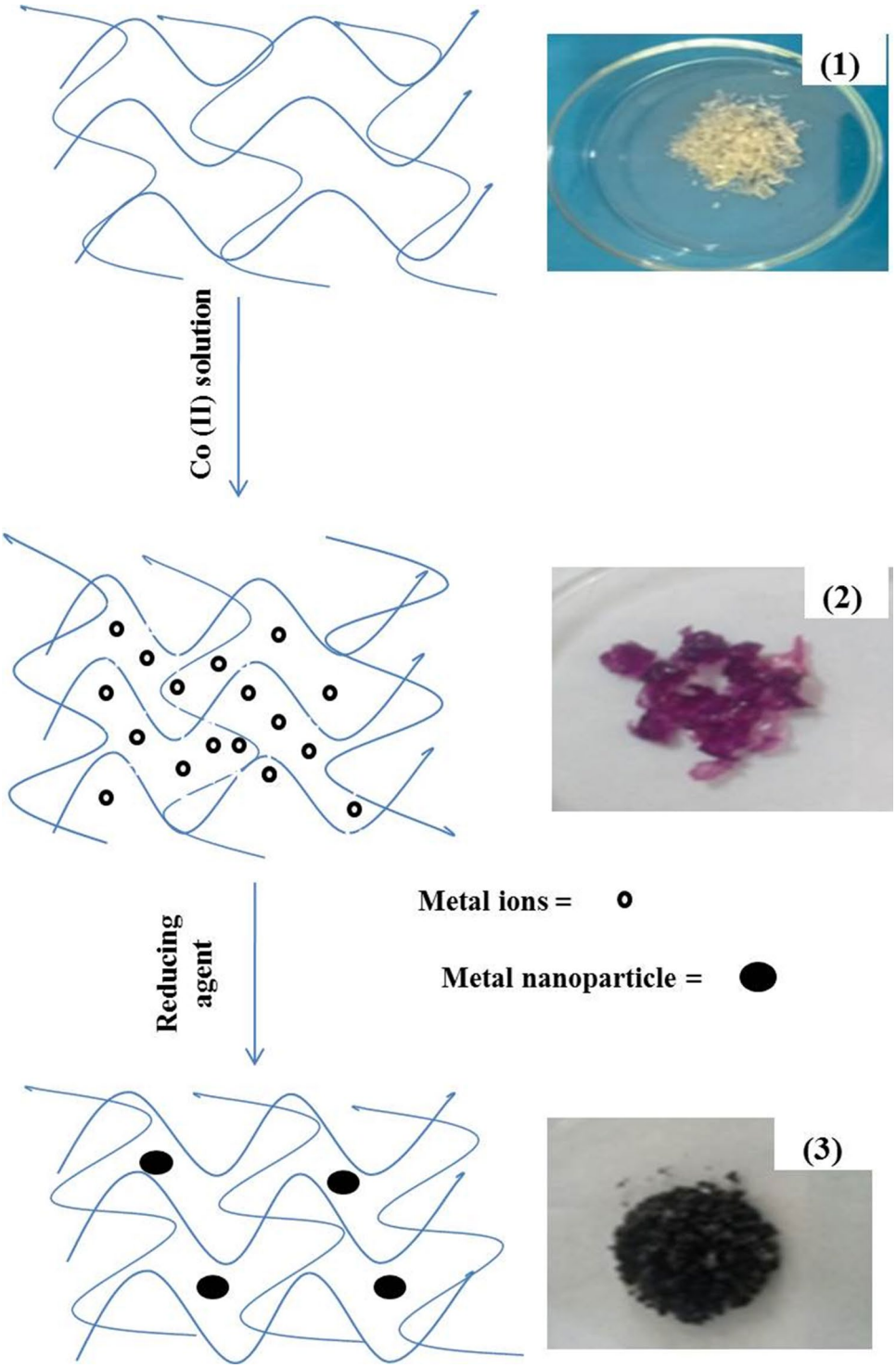

Fig. 1 Schematic representation for the synthesis of p(AAc)-Co composite and digital camera images of hydrogels loaded with (2) Co (II) and (3) Co nanoparticles

Catalytic activity

A very well-known reaction i.e., conversion of 4-NP to 4-AP was selected as a model reaction to evaluate catalytic performance of Co nanoparticles containing composite hydrogel. Pervious literature showed that mild reducing agents like $NaBH_4$ cannot reduce 4-NP into 4-AP without any catalyst. Therefore, newly prepared composite hydrogel can be used to testify its catalytic performance against this reaction. The study of this reaction is also very significant from environmental view point as it involves the degradation of 4-NP which is considered as highly toxic pollutant. Secondly, the reduction product i.e., 4-AP is very important in synthesis of different drugs such as

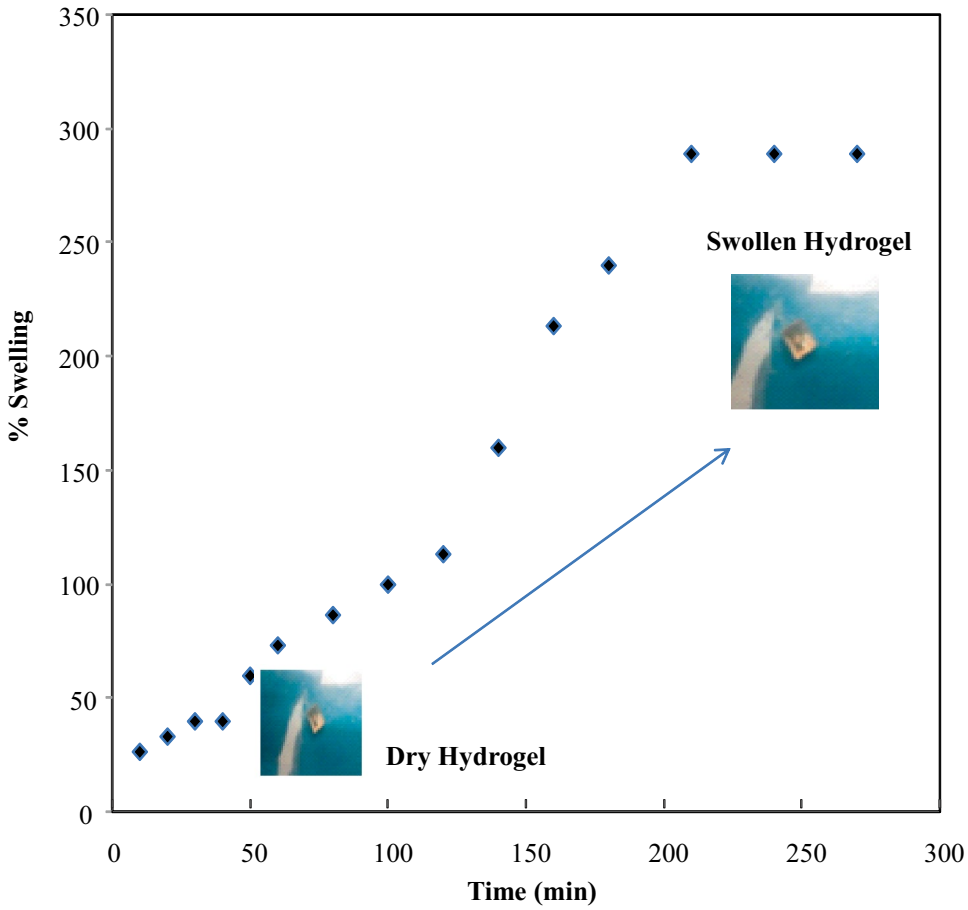

Fig. 2 The % swelling of p(AAc) hydrogel as a function of time and digital camera images p(AAc) hydrogel in dried and swollen forms

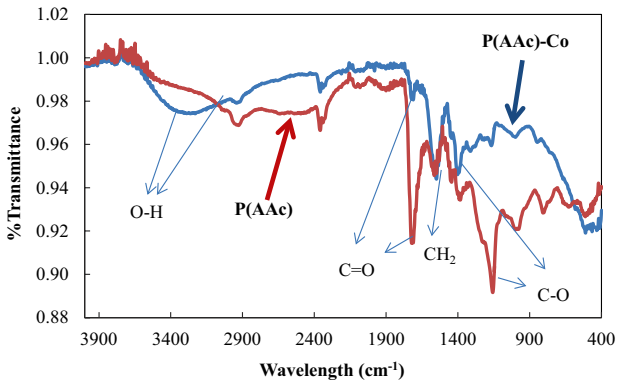

Fig. 3 FT-IR spectra of p(AAc) hydrogel and p(AAc)-Co composite

phenacetin, paracetamol, etc. in pharmaceutical industry [26, 27]. So, the selection of this reaction has many fold advantages; investigation of catalytic activity of a catalyst, degradation of a pollutant and production of useful reagent from a dangerous pollutant. According to the literature, the wavelength of maximum absorption for 4-NP is 317 nm. Reducing agents like $NaBH_4$ shift this peak to 400 nm by forming phenolate ion. However, the reduction of nitrophenlate ion cannot be accomplished simply by treating

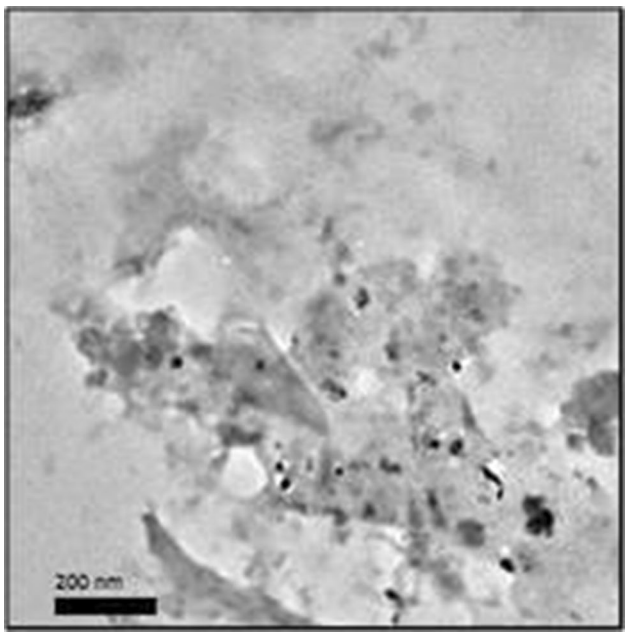

Fig. 4 TEM image of Co nanoparticles fabricated in p(AAc) hydrogel

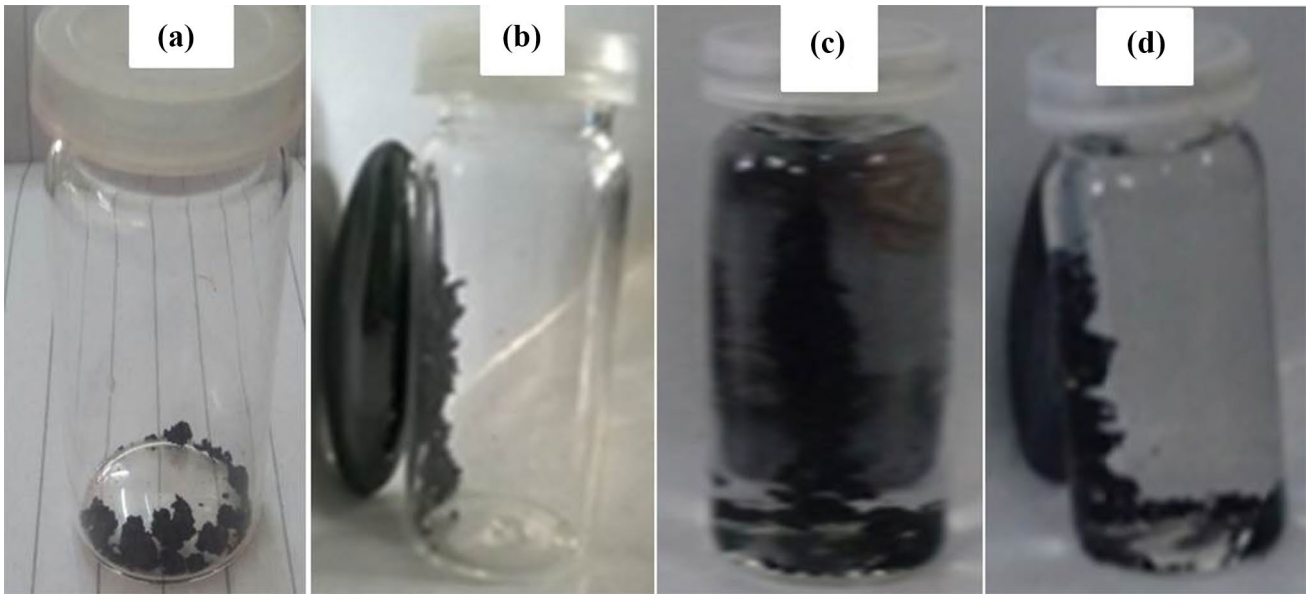

Fig. 5 Digital camera images of p(AAc)-Co composite, **a** dried composite in the absence of external magnetic field, **b** attraction of dried composite toward magnet, **c** composite suspended in water in the absence of external magnetic field, **d** movement of composite in water toward magnet

it with $NaBH_4$ in the absence of any outside assistance in the form of catalyst. The present work emphases on the use of newly prepared p(AAc)-Co composite catalyst to speed up the reaction rate in the reduction of 4-NP into 4-AP with $NaBH_4$ as reducing agent. As the reaction progresses, absorbance peak of 4-NP at 400 nm decreases gradually along with the appearance of another absorption peak at 300 nm representing the formation of 4-AP; the product of reduction reaction. UV–Visible spectra showing decrease in absorption intensity of 4-NP at 400 nm and increase in absorption peak of 4-AP at 300 nm is shown in Fig. 6. The two reactants, i.e., 4-NP and $NaBH_4$, are involved in the reaction; however, $NaBH_4$ was taken in large excess (100 times greater as compared to 4-NP) so the reaction was assumed to be independent of one reactant, i.e., $NaBH_4$. This large excess of $NaBH_4$ makes the reduction reaction to follow pseudo first order kinetics. So, the pseudo first order kinetic model (Eq. 2) was applied to calculate the rate constant value

$$\ln \frac{A_t}{A_o} = -k_{\text{app}} .t \tag{2}$$

In the above expression, the terms A_o and A_t represent the absorbance of 4-NP before reduction and at any time t during the course of reaction, respectively. The term k_{app} stands for apparent rate constant for the reduction of 4-NP and t is the time at which concentration C_t is observed. The rate of reaction for the reduction of 4-NP was determined in terms of k_{app} which was calculated from the slope of

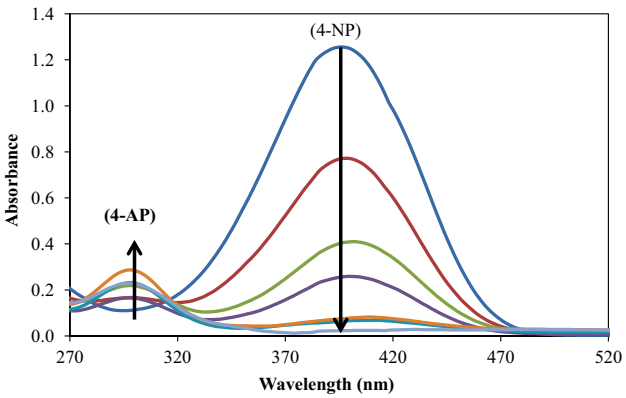

Fig. 6 UV-Visible Spectra for the reduction of 4-NP into 4-AP. Reaction Conditions: 0.001 M 4-NP = 50 ml, $NaBH_4$ = 0.19 g, p(AAc)-Co = 0.03 g, 250 rpm, 30 °C

the plot of $\ln(A_t/A_o)$ verses time t. A straight line graph with negative slope has been shown in Fig. 7. It was found that the rate constant was equal to 0.1718 min^{-1}. For the determination of E_a, the reduction of 4-NP was carried out at 30 °C and 60 °C. A value of rate constant as higher as 0.2384 min^{-1} was observed at 60 °C which is remarkably high as compared to the recently reported activity of Ni nanoparticles prepared using chitosan-silica and graphene oxide as templates by Ali et al. [28] and Qiu et al. [29], respectively. The apparent rate constants calculated for the reduction of 4-NP at these two different temperatures were utilized for the calculation of E_a from Arrhenius Equation (Eq. 3). The calculated activation energy was 9.24 kJ/mol.

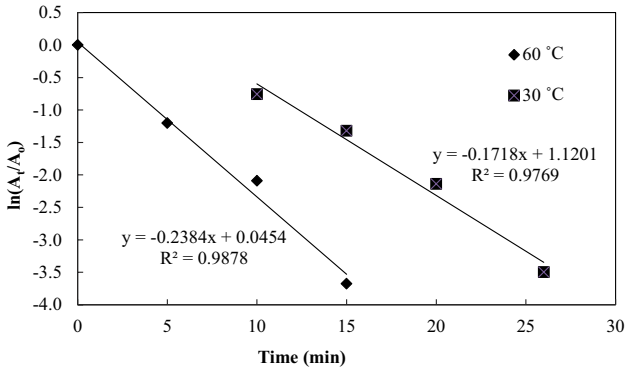

Fig. 7 Plots of $\ln(A_t/A_o)$ versus time for the reduction of 4-NP catalyzed by p(AAc)-Co composite. Reaction conditions; 0.001 M 4-NP = 50 ml, $NABH_4$ = 0.19 g, catalyst = 0.03 g, 250 rpm

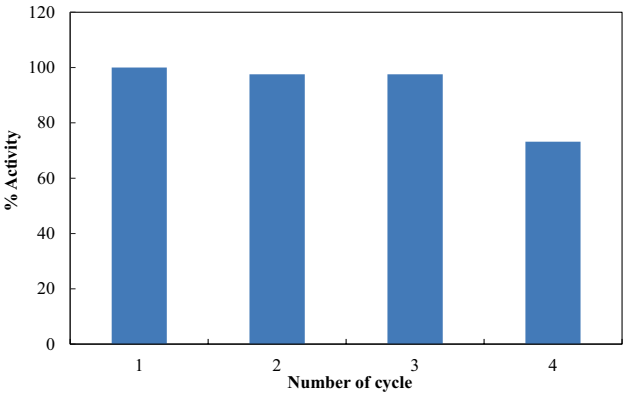

Fig. 8 Effect of recycling on catalytic activity in terms % activity of p(AAc)-Co composite catalyst as a function of number of cycle. Reaction conditions; 0.001 M NP = 50 ml, $NaBH_4$ = 0.19 g, Catalyst = 0.03 g of Co, 250 rpm, 30 °C

$$\ln\left(\frac{k_1}{k_2}\right) = \frac{E_a}{R}\left(\frac{1}{T_2} - \frac{1}{T_1}\right) \quad (3)$$

Recycling efficiency is a worth considering feature of a catalyst from economical view point. In order to make present work more applicable on industrial scale, recycling study of Co nanocatalysts entangled in p(AAc) networks was also carried out. This task was accomplished by employing p(AAc)-Co composite as catalyst for the reduction of 4-NP up to four consecutive cycles. For this, composite was removed out of the reaction medium after catalysis by filtration, followed by washing with distilled water and was applied as catalyst again for the same reaction under the same set of conditions. Plankton cloth filter was effectively used for the filtration process. Change in activity of catalyst was monitored with every cycle and is shown in Fig. 8. A decrease of 19% in catalytic activity of composite hydrogel containing Co nanoparticles was observed when it was used as catalyst in fourth consecutive cycle. This loss in catalytic activity can occur because of the conversion of metal atoms to metal oxides at the surface of nanoparticles or due to loss of some loosely entangled metal nanoparticles from hydrogel network. The loss of metal nanoparticles form the hydrogel network decreases the catalytic sites in hydrogel networks which in turn reduces the catalytic performance of the catalyst.

Adsorption study

In order to study the adsorption characteristics of p(AAc) hydrogel and its composite with Co nanoparticles, the process of elimination of MB from aqueous medium by adsorption using p(AAc) hydrogel and its composite with Co nanoparticles was chosen. MB solutions of different concentrations; 50, 100, 200, 250, 400, and 800 ppm were prepared and a fixed quantity (0.05 g) of the bare hydrogel was added into 100 ml solution of each concentration. The MB solutions containing adsorbent were gently stirred to allow the accumulation of MB on polymer chains of bare hydrogel networks. For the determination of quantity of MB attached on bare hydrogel with time in the process of adsorption, the sample was withdrawn from the reaction medium and amount of MB attached on bare hydrogel was determined by UV–Vis spectrometer. Figure 9a shows the increase in the adsorbed quantity of MB on per gram of p(AAc) hydrogel from each different concentrated solutions with the passage of time. A tremendous increase in the quantity of MB adsorbed on our bare hydrogel was detected when the initial concentration of MB solution was increased from 50 to 800 ppm. This increase in the adsorbed amount was observed because of greater availability of MB molecules in the adsorption medium. The maximum observed adsorption capacity of p(AAc) for MB was 836.5 mg/g which was achieved in 50 min of contact time. It is to worth mention that this adsorption rate and capacity is very high as compared to the recently published reports [30–32]. Figure 9b illustrates the % removal of MB from the aqueous solution of different concentrations of MB. For each concentration, the % removal was increased gradually with time and reached to maximum in 40 to 60 min depending upon the concentration of solution.

Adsorption isotherms

Adsorption isotherm is a graphical relationship between amount of adsorbate that is accumulated on the adsorbent and concentration of adsorbate solution provided that the adsorption process is carried out at constant temperature. Various adsorption isotherms have been developed to take into account the effects of different factors which can affect the adsorption capacity, adsorption rate and equilibrium

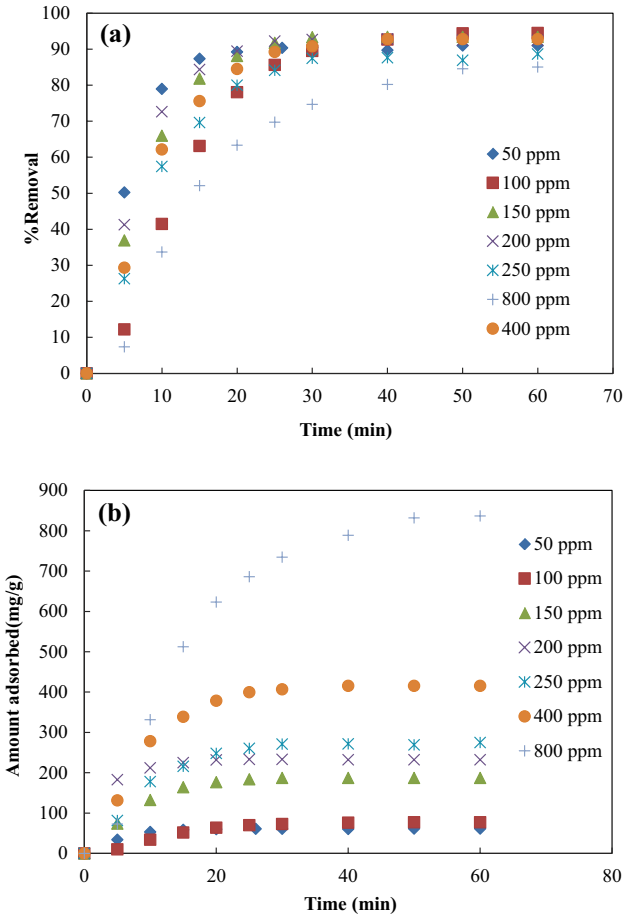

Fig. 9 **a** Amount of MB adsorbed on p(AAc) hydrogel with different concentrations. **b** Percentage removal of MB as a function of time with different concentrations of MB

state. Therefore, the application of adsorption isotherms is helpful to get insights of the adsorption process that may in turn be useful to understand the mechanism of adsorption process. A very famous adsorption isotherm which assumes that adsorbate is attached with adsorbent by a physical interaction and all the adsorption sites are identical and therefore each adsorption site has equal affinity for adsorbent molecules. This isotherm further assumes that each adsorption site can accommodate only one adsorbate molecule resulting in the establishment of a single layer of adsorbate on adsorbent surface. The isotherm based on these assumptions is known as Langmuir adsorption isotherm. It has been recently reported by Azizian et al. [33] that mathematical derivation of Langmuir isotherm model ignores the effect of adsorbate in desorption medium. Considering the effect of concentration of adsorbate in the desorption medium, Azizian and coworkers have introduced a modified Langmuir isotherm. The Langmuir isotherm eliminates the possibility of any roughness on the adsorbent surface, non-identical adsorption sites and the formation of multilayer of adsorbate molecules on adsorbent surface. However, the existence of these features cannot be neglected and taken into account by another adsorption isotherm which is known as Freundlich adsorption isotherm. The interaction between adsorbate molecules and adsorbent sites may also influence the adsorption parameters. This interaction is considered by Temkin adsorption isotherm according to which heat of adsorption of all molecules in the adsorption layer decreases linearly as the molecules of adsorbate adsorbed on the adsorbent increase and it is observed to a possible mutual interaction of adsorbate and adsorbent. The linear forms of the mathematical expressions of above-mentioned isotherms are given by Eqs. (4)–(7).

$$\text{Langmuir adsorption isotherm} \quad \frac{C_e}{q_e} = \frac{C_e}{q_m} + \frac{1}{q_m K_L} \tag{4}$$

$$\text{Modified Langmuir isotherm} \quad \frac{C_e}{q_e} = \frac{C_s}{q_m K_{ML}} + \frac{(K_{ML}-1)C_e}{q_m K_{ML}} \tag{5}$$

$$\text{Freundlich adsorption isotherm} \quad \ln q_e = \ln K_F + \frac{1}{n} \ln C_e \tag{6}$$

$$\text{Temkin adsorption isotherm} \quad q_e = B \ln K_T + B \ln C_e \tag{7}$$

where, for the present work, C_e is concentration of MB solution at equilibrium state of adsorption, C_s is the saturated concentration of MB solution, q_e is amount of MB in mg adsorbed per gram of p(AAc). The term q_m represents the maximum adsorption capacity of p(AAc) for MB from its aqueous solution and K_L is adsorption constant for Langmuir adsorption isotherm, K_{ML} is adsorption constant for the modified Langmuir adsorption isotherm. As the mathematical forms represent, both the Langmuir and modified Langmuir isotherm generate same graphical form which was obtained by plotting C_e/q_e versus C_e as shown in Fig. 10a. As it is clear from this plot, the nonlinear pattern was observed for both the Langmuir and modified Langmuir isotherm applied on the adsorption of MB on p(AAc). The determination of coefficient (R^2) for this isotherm was 0.751 which is far away from 1. The value of R^2 suggested that MB was not adsorb on the p(AAc) hydrogel in monolayer form. The Freundlich adsorption isotherm was plotted between ln C_e and ln q_e as shown in Fig. 10b. The value of R^2 obtained from the plot of Freundlich isotherm was 0.947 which was close to 1 and indicated that the adsorption of MB followed the Freundlich adsorption isotherm. The slope of Freundlich isotherm, $1/n$, provides information about nature of bonds between adsorbate and adsorbent. $1/n$ value between 0 and 1 represents the chemisorption. Furthermore, the value of $1/n$ in the range of 0.7 to 1 shows that by increasing the concentration of adsorbate solution the relative adsorption is decreased. This happens to the saturation of adsorption sites available

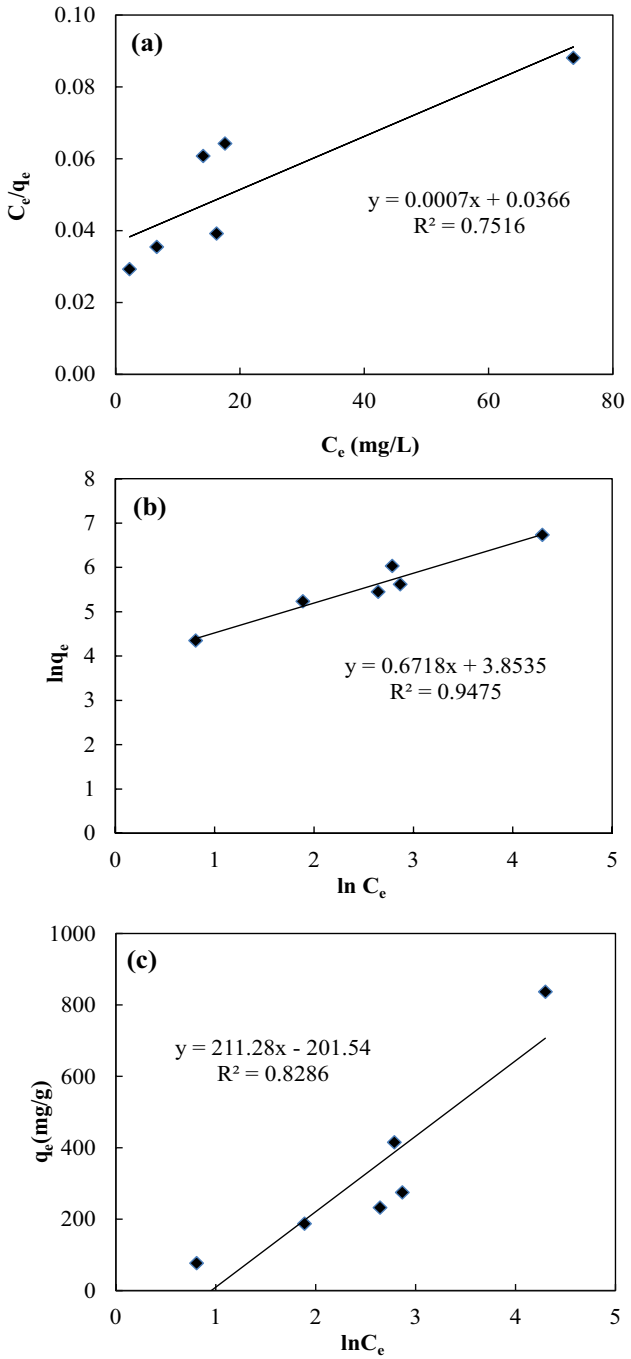

Fig. 10 Application of **a** Langmuir/modified Langmuir, **b** Fruendlich and **c** Temkin adsorption isotherm for the adsorption of MB onto the p(AAc) hydrogel. Reaction conditions; MB solution (50–800 ppm) = 100 ml, p(AAc) = 0.05 g, room temperature, 250 rpm

to adsorbate. Additionally, the value of 1/*n* also gives an idea about heterogeneity on adsorbent surface. If the value of 1/*n* is between 0 and 1, it indicates the chemisorption and the presence of heterogeneity on adsorbent surface and closer is the value of 1/*n* to 0 greater is the heterogeneity on adsorbent surface [34]. In the present work, the value of 1/*n* was equal to 0.6718 as given in Table 1 and shows that the process was chemisorption. This value is close to 1 as compared to 0 and hence indicating that the surface of adsorbent was heterogeneous but the degree of heterogeneity may be low. The graphical form of Temkin adsorption isotherm was obtained by plotting q_e as a function of ln C_e, and is shown in Fig. 10c. The value of R^2 was 0.828 which is far away from 1. The nonlinear pattern of Temkin adsorption isotherm showed that adsorption of MB was not followed by Temkin adsorption isotherm. The application of above four isotherms revealed that the adsorption of MB on p(AAc) can be best interpterted by Freundlich model. Kinetic parameters calculated from the applied adsorption isotherms are given in Table 1.

Comparison of adsorption capacity of bare composite hydrogel

The effect of fabrication of Co nanoparticles on the adsorption capacity of the prepared hydrogel was also studied. Equivalent amounts of the bare and composite hydrogel were added in aqueous solutions of MB having equivalent concentration and volumes. The amounts of MB adsorbed on both the bare and composite hydrogel adsorbents were plotted as a function of time and are shown in Fig. 11. It is clear that the rates of adsorption were almost similar in case of bare and composite hydrogel. However, a slight increment in the amount of MB adsorbed on composite hydrogel was observed. Actually, the MB was also adsorbed by the surface of Co nanoparticles due to their high surface energy. The increase in capacity of composite hydrogel to adsorb MB can be attained due to the higher affinity of Co nanoparticles for MB. The ability of magnetic composite hydrogel to retain its magnetic characteristics has been shown in Fig. 11b with digital camera images. Image (1) shows that particles of p(AAc)-Co composite remain suspended in aqueous solution of MB in the absence of any external magnetic field while the image (2) represents that composite attracted toward the externally applied magnetic field. The attraction of p(AAc)-Co composite particles after adsorption of MB toward the externally applied magnetic field demonstrates that p(AAc)-Co composite possess strong magnetic characteristics which were retained even after the adsorption of MB. This strong magnetic character of p(AAc)-Co offers an easy and simple way of removal of adsorbent after completing the adsorption task. In addition, the strong magnetic characteristics of the composite hydrogel can be utilized to tune the adsorption rate during the adsorption process by applying varying external magnetic field from outside the adsorption medium. So the fabrication of Co nanoparticles in p(AAc) hydrogel not only imparts magnetic characteristics but also increases its adsorption capacity and provides and alternate, easy and

Table 1 Kinetic parameters calculated from different adsorption isotherms applied for the adsorption of MB. Reaction conditions; MB solution (50–800 ppm) = 100 ml, p(AAc) = 0.05 g, room temperature, 250 rpm

Langmuir isotherm constants			Freundlich isotherm constants			Temkin isotherm constants			Modified Langmuir isotherm constants		
K_L (l/g)	q_m (mg/g)	R^2	K_F (l/g)	n	R^2	K_T (l/g)	B	R^2	K_{ML}	q_m (mg/g)	R^2
0.019	1428.57	0.751	47.134	1.488	0.947	0.385	211.3	0.828	834.88	1426.86	0.751

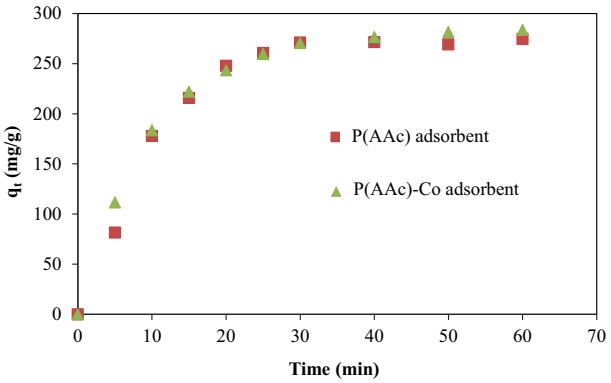

Fig. 11 Plots of amount of MB adsorbed on per gram of on p(AAc) hydrogel and on magnetic p(AAc)-Co hydrogel composite as a function of time. Reaction conditions adsorbent 0.05 g, 250 ppm MB solution 100 ml, 250 rpm, room temperature

economical way of removal of p(AAc)-Co adsorbent from aqueous adsorption medium.

Conclusions

Synthesis of p(AAc) hydrogel was accomplished by free radical polymerization. The synthesized hydrogel was used as a carrier system for magnetic Co nanoparticles synthesized by in situ chemical reduction treatment. The p(AAc) hydrogel matrix was found to have potential to control the aggregation of in situ fabricated Co nanoparticles. The p(AAc) hydrogels fabricated with Co nanoparticles exhibited strong magnetic properties. A very large amount of MB equivalent to 836.5 mg was adsorbed/gram of p(AAc) from aqueous medium. The adsorption equilibrium was attained within 60 min of contact time. Adsorption capacity of hydrogel was increased slightly after the fabrication of Co nanoparticles. Besides having potential to act as adsorbent, the p(AAc)-Co hydrogel composite was also found to possess catalytic activity. The p(AAc)-Co hydrogel composite showed good catalytic activity for 4-NP reduction reaction. The rate constant for the reduction of 4-NP catalyzed by p(AAc)-Co hydrogel composite catalyst was 0.238 min^{-1} and activation energy was 9.24 kJ/mol. Recycling of the magnetic poly(acrylic acid) hydrogel fabricated with cobalt nanoparticles was carried out for four consecutive cycles and 19% loss in catalytic activity was observed.

References

1. H. Li, P. Yang, P. Pageni, C. Tang, Macromol. Rapid Commun. **38**, 1700109 (2017)
2. C. Siangsanoh, S. Ummartyotin, K. Sathirakul, P. Rojanapanthu, W. Treesuppharat, J. Mol. Liq. **256**, 90 (2018)
3. M. Ghorbanloo, S. Tarasi, Lett. Drug Des. Discov. **14**, 605 (2017)
4. E.A. Kamoun, X. Chen, M.S.M. Eldin, E.-R.S. Kenawy, Arab. J. Chem. **8**, 1 (2015)
5. J.-H. Lee, H.-W. Kim, J. Tissue Eng. **9**, 2041731418768285 (2018)
6. R. Begum, K. Naseem, Z.H. Farooqi, J. Sol-Gel. Sci. Technol. **77**, 497 (2016)
7. N. Sahiner, Prog. Polym. Sci. **38**, 1329 (2013)
8. M. Ajmal, Z.H. Farooqi, M. Siddiq, Korean J. Chem. Eng. **30**, 2030 (2013)
9. R. Begum, Z.H. Farooqi, E. Ahmed, K. Naseem, S. Ashraf, A. Sharif, R. Rehan, Appl. Organomet. Chem. **31**, 3563 (2017)
10. Z.H. Farooqi, A. Ijaz, R. Begum, K. Naseem, M. Usman, M. Ajmal, U. Saeed, Polym. Compos. **39**, 645 (2018)
11. Z. Farooqi, S. Khan, R. Begum, Mater. Sci. Technol. **33**, 129 (2017)
12. S. Thakur, P.P. Govender, M.A. Mamo, S. Tamulevicius, V.K. Thakur, Vacuum **146**, 396 (2017)
13. C. Ao, R. Hu, J. Zhao, X. Zhang, Q. Li, T. Xia, W. Zhang, C. Lu, Chem. Eng. J. **338**, 271 (2018)
14. M. Ghorbanloo, N. Moharramkhani, T.M. Yazdely, H.H. Monfared, J. Porous Mater. **1**, 433 (2018)
15. Z.H. Farooqi, S.R. Khan, T. Hussain, R. Begum, K. Ejaz, S. Majeed, M. Ajmal, F. Kanwal, M. Siddiq, Korean J. Chem. Eng. **31**, 1674 (2014)
16. M. Ghorbanloo, A. Heydari, H. Yahiro, Desalin. Water Treat. **115**, 106 (2018)
17. M. Ghorbanloo, A. Heydari, H. Yahiro, Appl. Organomet. Chem. **32**, e3917 (2018)
18. Z.H. Farooqi, S.R. Khan, R. Begum, F. Kanwal, A. Sharif, E. Ahmed, S. Majeed, K. Ejaz, A. Ijaz, Turk. J. Chem. **39**, 96 (2015)
19. M. Ajmal, M. Siddiq, H. Al-Lohedan, N. Sahiner, RSC Adv. **4**, 59562 (2014)
20. S.B. Sengel, N. Sahiner, Eur. Polymer J. **75**, 264 (2016)
21. M. Ajmal, M. Siddiq, N. Aktas, N. Sahiner, RSC Adv. **5**, 43873 (2015)
22. S. Kang, Y. Zhao, W. Wang, T. Zhang, T. Chen, H. Yi, F. Rao, S. Song, Appl. Surf. Sci. **448**, 203 (2018)
23. F. Seven, N. Sahiner, J. Appl. Polymer Sci. **131**, 41106 (2014)
24. M. Ajmal, F. Aftab, I. Bibi, M. Iqbal, J. Ambreen, H.B. Ahmad, N. Akhtar, A. Haleem, M. Siddiq, J. Porous Mater. **26**, 281 (2019)
25. F. Bibi, M. Ajmal, F. Naseer, Z. Farooqi, M. Siddiq, Int. J. Environ. Sci. Technol. **15**, 863 (2018)

26. T. Komatsu, T. Hirose, Appl. Catal. A **276**, 95 (2004)
27. S. Wang, Y. Ma, Y. Wang, W. Xue, X. Zhao, J. Chem. Technol. Biotechnol. **83**, 1466 (2008)
28. F. Ali, S.B. Khan, T. Kamal, K.A. Alamry, E.M. Bakhsh, A.M. Asiri, T.R. Sobahi, Carbohyd. Polym. **192**, 217 (2018)
29. H. Qiu, F. Qiu, X. Han, J. Li, J. Yang, Appl. Surf. Sci. **407**, 509 (2017)
30. L. Chen, Y. Li, S. Hu, J. Sun, Q. Du, X. Yang, Q. Ji, Z. Wang, D. Wang, Y. Xia, J. Exp. Nanosci. **11**, 1156 (2016)
31. S.-T. Yang, S. Chen, Y. Chang, A. Cao, Y. Liu, H. Wang, J. Colloid Interface Sci. **359**, 24 (2011)
32. E. Altintig, H. Altundag, M. Tuzen, A. Sari, Chem. Eng. Res. Des. **122**, 151 (2017)
33. S. Azizian, S. Eris, L.D. Wilson, Chem. Phys. **513**, 99 (2018)
34. A. de Sá, A.S. Abreu, I. Moura, A.V. Machado, Polymeric materials for metal sorption from hydric resources, in *Water Purification*, ed. By A. Grumezescu (Elsevier, 2017), p. 289